Follicular lymphoma cell niche: identification of a preeminent IL-4-dependent T(FH)-B cell axis

Céline Pangault [1 2 #], Patricia Amé-Thomas [1 2 #], Philippe Ruminy [3], Delphine Rossille [4], Gersende Caron [1 2], Maryse Baia [5 6], John De Vos [7], Mikael Roussel [2], Céline Monvoisin [1], Thierry Lamy [1 8], Hervé Tilly [3 9], Philippe Gaulard [5 6], Karin Tarte [1 2 *], Thierry Fest [1 2 *]

[1] *Microenvironnement et cancer INSERM : U917 , IFR140 , Université de Rennes I , FR*

[2] *Service d'anatomie et cytologie pathologiques CHU Rennes , Hôpital Pontchaillou , FR*

[3] *Groupe d'étude des proliférations lymphoïdes INSERM : U918 , Université de Rouen , Rouen,FR*

[4] *Modélisation Conceptuelle des Connaissances Biomédicales INSERM : U936 , IFR140 , Université de Rennes I , FR*

[5] *Institut Mondor de Recherche Biomédicale INSERM : U955 , Université Paris XII Val de Marne , IFR10 , FR*

[6] *Service d'anatomie pathologique Assistance publique - Hôpitaux de Paris (AP-HP) , Hôpital Henri Mondor , Université Paris XII Val de Marne , Créteil,FR*

[7] *IRB, Institut de recherche en biothérapie CHRU Montpellier , Université Montpellier I , Hôpital Saint-Eloi 34000 Montpellier,FR*

[8] *Service d'hématologie clinique CHU Rennes , Hôpital Pontchaillou , Université de Rennes I , FR*

[9] *Département d'Hématologie CRLCC Henri Becquerel , Rouen,FR*

* K.T. and T.F. contributed equally to this work and are co-corresponding authors <karin.tarte@univ-rennes1.fr >, <thierry.fest@univ-rennes1.fr >

# C.P. and P.A-T. contributed equally to this work

Abstract

Follicular lymphoma (FL) B cells contract tight connections with their microenvironment, which governs the pathogenesis and progression of the disease. Indeed, specific immune response gene signatures, obtained on whole biopsy samples, have been associated with patient survival. In this study we performed gene expression profiling of purified B-cell and non-B cell compartments obtained from FL and reactive lymph nodes. We identified 677 nonredundant genes defining the FL interface and involving 26 FL-specific functional networks. This approach highlighted an IL-4-centered pathway associated with an activation of STAT6 that favors overexpression of IL-4-target genes. In addition, FL microenvironment was characterized by a strong enrichment in follicular helper T cells (T_{FH}), as demonstrated through transcriptomic and flow cytometry analyses. The majority of phospho-STAT6^{pos} B cells were located at the vicinity of cells expressing the PD-1 T_{FH} marker. Moreover, purified FL-derived T_{FH}, expressed *IL4* at very high levels compared to purified tonsil-derived T_{FH} or non-T_{FH} microenvironment. Altogether, our study demonstrated that tumor-infiltrating T_{FH} specifically express functional IL-4 in FL, creating an IL-4-dependent T_{FH}-B cell axis. This crosstalk could sustain FL pathogenesis and represent a new potential therapeutic target.

MESH Keywords B-Lymphocytes ; physiology ; Cell Communication ; Cell Separation ; methods ; Gene Expression Profiling ; Humans ; Interleukin-4 ; physiology ; Lymphocyte Activation ; Lymphocytes, Tumor-Infiltrating ; physiology ; Lymphoma, Follicular ; etiology ; immunology ; Oligonucleotide Array Sequence Analysis ; STAT6 Transcription Factor ; physiology ; T-Lymphocytes, Helper-Inducer ; physiology

Author Keywords follicular lymphoma ; follicular helper T cells ; microenvironment, IL-4

INTRODUCTION

Follicular lymphoma (FL) is the most common indolent non-Hodgkin's lymphoma and remains virtually incurable. FL tumors arise from germinal center (GC) B cells and are characterized by the balanced chromosomal translocation t(14;18) leading to the deregulation of *BCL2* expression.1 Occurring in about 85% of FL cases, this *BCL2-JH* translocation was also detected in a small proportion of circulating atypical B cells in healthy individuals, that represent potential premalignant intermediates of the FL pathogenesis.2 Therefore, translocated *BCL2* gene is not sufficient *per se* to drive FL development, thus predicting the existence of additional genetic and/or environmental factors crucial for lymphomagenesis and clinical behavior. Several studies argue for FL as a disease under the dependency of strong interactions between tumor B cells and their microenvironment. Both stromal cells and CD40L signal efficiently promoted the survival of FL B-cells *in vitro.* 3 ,4 In addition, within invaded lymph nodes (LN) and bone marrow, malignant B cells are found admixed with specialized stromal cells, including follicular dendritic cells, and CD4^{pos} T cells, thus mimicking the normal GC organization.1 Interestingly, CD4^{pos} T cells in the follicles, called follicular helper T cells (T_{FH}), were recently suggested to constitute a distinct lineage of T helper cells that arises independently of Th1, Th2, and Th17 effector subsets, and is required for normal B-cell selection and differentiation into long-lived plasma cells.5 –7 However, no studies have addressed to date the role of T_{FH} in FL pathogenesis. The cellular composition of the non-malignant infiltrate was described as related to FL prognosis but these studies have often generated

conflicting results. High numbers of $CD7^{pos}$, $CD4^{pos}$, $Foxp3^{pos}$, and $PD\text{-}1^{pos}$ T-cells were successively reported to predict a longer survival in FL patients.8 –11 Moreover, the spatial distribution, rather than a numerical change, of non-malignant cells seems to be important, since a perifollicular location of $Foxp3^{pos}$ T cells was associated with a better prognosis8 whereas FL with rapid transformation showed a predominantly intrafollicular $CD4^{pos}$ pattern of expression.12 However, these results remain controversial and a range of commonly used T-cell markers fail to identify a significant association with overall survival.8 ,13 Other studies reported that a reactive environment infiltrated by a low number of $CD8^{pos}$ T cells14 or a high content of $CD68^{pos}$ or $CD163^{pos}$ macrophages9 ,13 or mast cells15 was associated with adverse clinicobiologic manifestations and unfavorable outcome in FL patients that were treated with conventional chemotherapy. Of note, the predictive value of microenvironment cell populations in FL is highly dependent on specific treatment protocols.16 ,17 To draw a more complete picture of the influence of the microenvironment in FL, microarray analyses were performed and allowed to identify two specific molecular signatures associated with patient's outcome independently of classical clinical features.18 One was associated with a favorable outcome and corresponded to T cell- and monocyte-restricted genes; whereas the other one involved genes expressed by activated macrophages and dendritic cells and was associated with an adverse prognosis. Subsequent papers confirmed that the clinical behavior in FL is determined essentially by the gene expression profile of the microenvironment rather than by inherent properties of tumor cells themselves.19 ,20 However, the specific contribution of the non-malignant compartment has never been addressed in these retrospective studies.

To better understand the host-tumor interaction in FL, we performed comprehensive gene expression analyses on purified B-cell and non-B cell compartments of tumor and reactive LN. This study enables to explore molecular crosstalk between tumor cells and tumor-infiltrating immune cells by identifying a specific list of genes involved in the FL interface. Among this list, we identified an IL-4-centered pathway and demonstrated that T_{FH} are expanded within invaded LN and are the major IL-4 producing cells in FL.

MATERIALS and METHODS

Patients and Samples

All tissues used for this study came from subjects recruited under institutional review board approval and informed consent process according to the Declaration of Helsinki. Samples were obtained either from freshly isolated LN from 29 patients with *de novo* FL at diagnosis, and 11 patients with reactive non-malignant disease (NEG) considered as normal counterpart, or from 11 human tonsils (TONS) collected from children undergoing routine tonsillectomy. All FL showed a predominantly follicular growth pattern, CD10 expression, and were classified into grades 1, 2, or 3a according to the WHO diagnostic criteria. Patients with FL grade 3b or with disease in relapse after treatment, as well as transformed FL were excluded. Clinical characteristics of FL patients are listed in supplementary Table S1 . Tissues were rapidly dissociated after collection and flushed using syringe and needle. Cell suspensions were then filtered and washed by centrifugation to obtain the unselected cell fraction.

Flow cytometry characterization of B and non-B subpopulations

Flow cytometry analyses of cell suspensions obtained after mechanically dissociation were performed on a Cytomics FC500 (Beckman Coulter, Miami, FL) or a FACSAria (Becton Dickinson, Franklin Lakes, NJ) flow cytometer using several cocktails of mAbs (Supplementary Table S2). Percentages of tumor B cells among $CD19^{pos}$ B cells were determined as $CD19^{pos}$ cells with a restricted expression of kappa or lambda light chain after subtraction of the expected percentage of normal B cells expressing this isotype.

Cell sorting

Purification of B ($CD19^{pos}$) and non-B ($CD19^{neg}$ $CD22^{neg}$) fractions was performed using a two-step magnetic bead cell-sorting. First, $CD19^{pos}$ B lymphocytes were obtained by positive selection using CD19 microbeads (StemCell Technologies, Vancouver, Canada). Residual B cells were then eliminated from the unbound fraction by a second round of depletion using CD22 microbeads (Miltenyi Biotec, Gladach, Germany), obtaining therefore the $CD19^{neg}$ $CD22^{neg}$ microenvironment compartment (Env). Purity of each fraction was assessed by flow cytometry on CD20 expression. $CD3^{pos}$ $CD4^{pos}$ $CXCR5^{hi}$ $ICOS^{hi}$ $CD25^{neg}$ T_{FH} and T_{FH} -depleted/B cell-depleted cell compartment (Env nonT_{FH}) were purified using a FACSAria cell sorter from tonsils and FL lymph nodes.

RNA extraction

Total RNA was extracted using AllPrep™ ARN/ADN mini kit (Qiagen, Valencia, CA), as recommended by the manufacturer including DNAse I treatment. RNA purity and integrity was assessed by capillary electrophoresis using the Bioanalyzer 2100 (Agilent, Santa Clara, CA) and the 2100 Expert software. All samples used for microarray studies displayed a RNA Integrity number (RIN) of at least 6.7 (mean: 9.2, range: 6.7–10).

Microarray hybridization

Microarray analyses were performed either on $CD19^{pos}$ fractions of 16 FL (FL_B) and 5 non-malignant (NEG_B) LN, or $CD19^{neg}$ $CD22^{neg}$ microenvironment fractions (8 FL_Env and 6 NEG_Env). Biotinylated cRNA were amplified according to the small sample

labeling protocol and hybridized on the GeneChip HG-U133 Plus 2.0 oligonucleotide arrays (Affymetrix, Santa Clara, CA), according to the manufacturer's instruction. Data analyses were performed using the ArrayAssist® software (Stratagene, La Jolla, CA, USA) (see supplementary data).

Real-time quantitative PCR (RQ-PCR)

Microarray results were confirmed by RQ-PCR on a set of 19 FL_Env, 8 NEG_Env, and 6 $CD19^{neg}$ $CD22^{neg}$ fractions obtained from tonsils (TONS_Env). Reverse transcription was performed on 1 μg of total RNA using the Superscript II reverse transcriptase and random hexamers (Invitrogen). On-demand gene expression assays and the Taqman Universal master mix on an ABI Prism 7000 Sequence Detection System (Applied Biosystems, Forster City, CA) were used for RQ-PCR. *ABL* was determined as the appropriate internal housekeeping gene. For each sample, the Ct value for the gene of interest was determined, normalized to its respective value of *ABL* and compared to the value obtained for NEG_Env, using the ΔCt method. For *IL4* mRNA expression, the median of FL_Env expression, evaluated by RQ-PCR, was 11.1 compared to NEG_Env (assigned to 1). We classified the FL cases according to *IL4* low ($IL4^{lo} < 10$) or high ($IL4^{hi} > 12$) relative expression. Statistical analyses were performed with Prism software (GraphPad software Inc, San Diego, CA) using a Mann-Whitney non-parametric U-test (**P* <0.05, ** *P* <0.01, *** *P* <0.001). In addition, *GCET2/HGAL* was explored on purified FL_B treated or not with IL-4 (R&D Systems, 10 ng/ml) whereas *IL4* was quantified on purified T_{FH} *versus* Env non T_{FH} obtained from both tonsils and FL.

Immunohistochemistry

Tonsils (n=3), reactive lymph nodes with follicular hyperplasia (n=7) and follicular lymphoma (n=12) biopsies were analyzed as previously described.21 Briefly, after appropriate antigen retrieval with microwave heating in high pH Target Retrieval Solution (DakoCytomation, Glostrup, Denmark), deparaffinized tissue sections were stained with anti-Phospho-STAT6/Tyr641 Ab (polyclonal rabbit, dilution 1/30, Cell Signaling Technology, Danvers, MA), using an indirect immunoperoxidase method (ImmPRESS anti-rabbit, Vector Laboratories, Burlingame) and diaminobenzidine (DAB, Vector Laboratories) as chromogen. For double immunostaining, slides were first incubated with anti-CD20 (clone L26, Dako), anti-CD5 (clone 4C7, Novocastra, Newcastle, UK) or anti-PD1 (clone NAT, Abcam, Cambridge, UK) mAb and labelled using the alkaline phosphatase – conjugated ABC procedure (Vector Laboratories). Naphtol phosphate fast red was used as chromogen (Sigma, Saint Louis, MO). Then, slides were incubated with anti-phospho-STAT6/Tyr641 and detected as described above. External positive controls included nodular sclerosis classical Hodgkin lymphomas as well as paraffin embedded blocks of L428 Hodgkin lymphoma-derived and MedB1 primary mediastinal B-cell lymphoma-derived cell lines. Images were captured with a Zeiss Axioskop2 microscope (Zeiss, Oberkochen, Germany) and Neofluar 100x/0.1 NA optical lenses (Zeiss). Photographs were taken with a DP70 Olympus camera (Olympus, Tokyo, Japan). Image acquisition was performed with Olympus DP Controller 2002, and images were processed with Adobe Photoshop v7.0 (Adobe Systems, San Jose, CA).

RESULTS

Validation of our cell sorting method

To validate our approach of cell separation, we analyzed by flow cytometry the different compartments before and after cell purification. Malignant B cells were evaluated on the basis of kappa/lambda (K/L) staining on $CD19^{pos}$ cells and, before cell sorting, represented more than 75% of the total cell count and 90% of B lymphocytes [median: 96.5%; range: 75–100]. After the two-step purification, B cell purity was at least 92% of the CD19-sorted fractions [median: 97%; range: 92–100], while the non-B-cell fractions were contaminated by less than 12% of $CD20^{pos}$ B cells [median: 0.7%; range: 0–12]. To further explore our cell purification method, we demonstrated, using tonsils samples, the unbiased enrichment of T cell subsets (Supplementary Figure S1), NK cells ($CD3^{neg}$ $CD16^{pos}$ $CD56^{pos}$), myeloid (Lin^{neg} HLA-DR^{pos} $CD11c^{pos}$) and plasmacytoid dendritic (Lin^{neg} HLA-DR^{pos} $CD123^{pos}$) cells in non-B cell fractions, whereas the kappa/lambda ratio was preserved in B cells (Supplementary Figure S1).

Microarray analysis of the FL specific interface

We used a microarray approach to characterize gene expression patterns in different purified subpopulations of 16 FL (16 FL_B and 8 FL_Env) and 6 non-malignant (NEG) LN (5 NEG_B and 6 NEG_Env). These 35 Samples were labeled and hybridized onto Affymetrix U133 Plus 2.0 oligonucleotide arrays. Raw data were normalized using GC-RMA method and filtered to select probesets (PS) with standard deviation to mean ratio superior to 80%. This method reduces the panel to 8779 PS showing the highest expression variation. Unsupervised analyses of either B-cell compartments (n=21) or non-B cell compartments (n=14) allowed to differentiate FL from NEG samples (Figure 1A). To determine the gene expression pattern specific to each cell compartment implicated in the host-tumor crosstalk, a step-wise statistical approach was conducted on the 35 samples by combining a SAM method and an asymptotic unpaired Mann-Whitney non-parametric test. Based on this approach, we defined four different PS lists (Figure 1B , Left Panel): 1) 886 PS differentially expressed between FL and normal B cells, representing the FL-specific B signature; 2) 897 PS differentially expressed between FL and normal non-B microenvironment, representing the FL-specific microenvironment signature; 3) 4127 PS distinguishing B and non-B FL samples (FL interface); and 4) 2308 PS distinguishing B and non-B reactive samples (normal interface). In order to define the specific host-tumor

interface, which contains genes specifically implicated in the crosstalk between tumor B cells and their microenvironment, we established two ways to select relevant PS. We first subtracted the normal interface signature (2308 PS) from the FL interface signature (4127 PS) ending therefore with a 2206 PS signature called FL specific interface-1. The second way consisted to sum the FL-specific B PS to the FL-specific microenvironment PS, allowing the definition of the FL specific interface-2 involving 1698 PS (Figure 1B , Middle Panel). Finally, the overlap merging between these two previous genelists involved 788 highly specific FL-interface PS corresponding to 677 non-redundant genes and characterizing what we further designed as the FL tumor-microenvironment specific interface (Figure 1B , Right Panel). Among this list, 219 PS were up-regulated in FL B cells and 569 PS up-regulated in FL non-B cell compartment (Table S3).

IL-4 is upregulated in FL and promotes malignant B-cell activation

Within the 788-PS list defining the FL specific interface, we identified, using Ingenuity pathway analysis, 26 FL-specific functional networks, including an IL-4 centered pathway, a cell growth and proliferation pathway, and an immune response pathway (Table S4). We pointed out that cell growth, T-lymphocyte proliferation and T-lymphocyte activation were altered in the FL microenvironment, with upregulation of *BATF*, *IFNRAR2, TNFRSF9, TRAF1*, *CCL4, IL10, IL15, IL4, TNRFRSF4,* or *TNFRSF18* gene expression. In addition, a Gene Ontology analysis of the 788-PS list confirmed a statistically significant overrepresentation of genes involved in the biological processes of lymphocyte proliferation (GO: 0042100, *P*= 0.00066) or lymphocyte activation (GO:0046649, *P* =0.00016), especially T-cell activation (GO:0042110, *P* =0.00011). According to the Onto-Tools pathway impact analysis, *IL4* was present in 6 out of the top 20 functional pathways relevant for the 788-PS list description. Moreover, we performed hierarchical clustering analysis based on the previously described immune-response 1 and 2 signatures.18 Of interest, the immune-response 1 segregated the FL_Env from the NEG_Env indicating a preferential T-cell signature in the FL cases (Figure S2). To further explore the T-cell implication in FL tumorogenesis and specifically through the IL-4 centered pathway, we first validated by RQ-PCR the overexpression of *IL4* mRNA in FL_Env, compared to NEG_Env (Figure 2A). Similarly, *IL4* was expressed at a very low level in non-B cell fraction from inflamed benign tonsils. The result confirmed the recently described higher levels of IL-4 protein in FL compared to benign follicular hyperplasia.22 In this previous study, activation of STAT6 was poorly detectable, probably due to the use of whole tissue lysates. Given that FL B cells, like normal GC-derived B cells, strongly expressed CD124, the IL-4 receptor alpha (Figure 2B), we decided to investigate the expression of activated phospho-STAT6 *in situ* by immunohistochemistry in malignant *versus* normal B cells. In reactive tonsils and lymph nodes (n= 10), only exceptional single cells positive for P-STAT6 (1 or 2 per section in magnification × 200) (Figure 2C , panel 1) were observed. These cells were located in the interfollicular area or in the mantle zone of follicles and were not observed within GC. In only one case of reactive lymph node, a cluster of P-STAT6^{pos} cells was found in the paracortex. By contrast, a high number of P-STAT6 positive cells was evidenced in all FL cases with interpretable staining (n=10), and were mainly located within the neoplastic follicles. These P-STAT6 positive cells consisted of either multiple scattered cells or small aggregates with a tendency of distribution at the periphery of malignant follicles (Figure 2C , panels 2 and 3). Double staining revealed that the P-STAT6 positive cells were CD20^{pos} B lymphocytes (Figure 2C , insert in panel 3. Of note, the level of STAT6 mRNA was not different between FL_B and NEG_B compartments (data not shown). Since IL-13 was not overexpressed in FL non-B cell compartments (data not shown), this phosphorylation of STAT6 is more likely to result from IL-4 than from IL-13. The overexpression of IL-4 within FL microenvironment was thus associated to a strong activation of malignant B cells. In agreement, we found that both *IL4I1* and *HOXC4* , two previously described IL-4 target genes,21 ,23 belonged to the 886-PS FL_B list (Supplementary Figure S3A). Similarly, *GCET2/HGAL* , another gene reported as induced by IL-4 in normal B cells and in some malignant B-cell lines,24 was significantly upregulated in FL_B compartment (Supplementary Figure S3B) even if it was excluded from the microarray analysis by the initial SD-based filtering. Interestingly, we demonstrated that *GCET2/HGAL* expression was also increased by IL-4 in purified primary B cells obtained from FL patients (Figure 2D).

IL-4 is predominantly produced by FL-derived T_{FH}

IL-4 is widely recognized as a Th2 cytokine in the periphery even if recent studies have suggested that, within reactive LN, T_{FH} are the main IL-4-secreting T cells, in agreement with the critical role of this cytokine for antibody production.7 ,25 –27 In order to identify the IL-4 producing cells in FL context, we first compared by RQ-PCR, in the microenvironnement of FL *versus* nonmalignant samples, the expression of *BCL6*, *GATA3,* and *TBX21/TBET* transcription factors, which are involved in the commitment to T_{FH} , Th2, and Th1 differentiation respectively. Both, the *BCL6* expression and the *GATA3/TBX21* ratio were increased in FL tumors, suggesting a simultaneous enrichment in T_{FH} and Th2-polarized CD4^{pos} T cells. In addition, *IL10*, the second prototypic Th2 cytokine, was also overexpressed in FL_Env (Figure S4A). Since T_{FH} also express low levels of GATA3,27 we decided to further explore the potential contribution of T_{FH} to FL pathogenesis through the synthesis of IL-4. First, a Gene Set Enrichment Analysis (GSEA) approach was used in order to specifically assess the over-representation of previously described T_{FH} genes within the FL microenvironment. Given the recent demonstration in both mice and human that CXCR5 and ICOS are the two most relevant T_{FH} phenotypic markers, we defined our T_{FH} signature based on the datasets previously published by Rasheed *et al.* , where CXCR5^{hi} ICOS^{hi} CD4^{pos} T cells were isolated from tonsils and compared, using Affymetrix U133A/B microarrays, to purified non-T_{FH} , naïve T cells, central memory T cells, and effector memory T cells.28 We underlined 326 PS significantly upregulated in T_{FH} cells compared to the other CD4^{pos} T-cell subpopulations and corresponding to 267 non-redundant genes. Having ranked the microenvironment cell samples according to FL *versus* NEG distinction, we

found that FL_Env were significantly enriched in genes specifically overexpressed in T_{FH} cells (P <0.01 using both SNR-based ranking and FC-based ranking) (Figure S4B). Interestingly, when we performed an unsupervised hierarchical clustering restricted to the 226 PS of the T_{FH} signature belonging to our initial dataset of 8879 PS, we were able to segregate FL cases from non-tumoral tissues (data not shown), indicating that the T_{FH} signature was sufficient by itself to distinguish the FL microenvironment from the non-malignant microenvironment. The cluster of coordinately regulated T_{FH} -associated genes was underlined in Figure 1A . Moreover, unsupervised analysis based on T_{FH} signature revealed the clustering of FL_Env according to their *IL4* mRNA expression level (Figure 3), providing additional evidence that IL-4 could be secreted by the T_{FH} compartment. Furthermore, we also found by GSEA analysis a significant enrichment of the T_{FH} signature in FL with high expression of $IL4^{hi}$ (*P<0.001* ; data not shown). In agreement, we validated by RQ-PCR the overexpression of *CXCL13, CXCR5* , and *PDCD1* , three canonical human T_{FH} markers, in FL_Env compared to NEG_Env (Figure S4C). In order to take into account the inflammatory process that develops within FL microenvironment, we decided to explore also the non-B cell compartment obtained from chronically activated tonsils. In fact, substantial differences were seen in the degree of GC compartmentalization between human lymph node GC and human tonsil GC, including an accumulation of GC T cells in the latter one.29 Interestingly, the level of expression of *CXCL13, CXCR5* , and *PDCD1* in tonsil microenvironment was also upregulated compared to normal LN in similar extent than FL LN. We then quantified by flow cytometry the percentage of $CD4^{pos}$ $CD25^{neg}$ T cells coexpressing high levels of CXCR5 and ICOS T_{FH} markers (Figure 4A) and found a significant expansion of the T_{FH} cell compartment, in both FL tumors and tonsils compared to normal LN (Figure 4B). Of note, the two reactive LN with higher percentages of T_{FH} corresponded to samples with a strong follicular hyperplasia. FL microenvironment is thus characterized, like samples with strong GC activation, by a high infiltration of T_{FH} cells. Within FL biopsies, P-$STAT6^{pos}$ B cells were found in close contact to $CD5^{pos}$ T cells and most of them were located at the vicinity of cells expressing the PD-1 T_{FH} marker (Figure 4C). Previously, it had been very difficult to identify IL-4 producing cells *in situ* 25 and T_{FH} are highly susceptible to apoptosis *in vitro.* 28 To definitively determine the IL-4 producing cells, we thus decided to purify the T_{FH} and the non-B non-T_{FH} cell subsets in FL and tonsils and to screen these cell compartments for *IL4* mRNA. *IL4* was highly produced by the T_{FH} fraction issued from FL compared to the other non-malignant cells of the microenvironment, whereas tonsil-derived T_{FH} expressed a low but significant level of *IL4* mRNA (Figure 4D). In addition, when considering more specifically the non-T_{FH} $CD4^{pos}$ $CXCR5^{neg}$ $ICOS^{neg}$ T cell subset, we confirmed that T_{FH} are the predominant *IL4* producing $CD4^{pos}$ T cells in FL (data not shown). Collectively, these results indicated that FL-infiltrating T_{FH} specifically produced very high levels of IL-4.

DISCUSSION

Follicular lymphoma represents a paradigm of microenvironment involvement in cancer behavior. Indeed, as previously described, the aggressiveness of the disease and the prognosis were carried by molecular features of non-malignant cells.18 Various studies have demonstrated the potential for using gene expression profiles for the assessment of tumor specific pathways. In order to explore the cellular crosstalk between lymphoma cells and their microenvironment, previous studies developed, in few biopsy samples, cell sorting experiments allowing the purification of both a $CD19^{pos}$ malignant and a $CD19^{neg}$ non-malignant subpopulations in order to validate some specific findings obtained by microarray on global tissues.18 To characterize the FL cell niche and molecular features that sustain tumor B-cell growth within a specific microenvironment, we carried out an exhaustive gene profiling study based on a validated purification method separating systematically fresh tumor cell suspension into $CD19^{pos}$ and $CD19^{neg}$ $CD22^{neg}$ compartments and we compared *de novo* FL to non-malignant LN.

Various genelists were generated leading to the definition of the FL interface as the specific host-tumor interface, including an IL-4-centered signature. We were able to identify by microarray the overexpression of *IL4* RNA in FL, demonstrating the better sensibility of our purification-based microarray approach compared to previous studies, ruling out the idea that for IL-4 no correlation may exist in FL between gene expression and protein levels.23 Of interest, although the size of our FL cohort and our study design did not allow the exploration of patient's prognosis in regard to gene profile, we found that the immune-response 1 described by Dave *et al.* could segregate the FL from the non-malignant microenvironment indicating a preferential T-cell signature among the FL cases.18 In addition, our FL specific interface showed a preferential expression of the CXCL13 chemokine in FL. Therefore both findings together suggest that the FL microenvironment retain features of the germinal center light zone.30 Whereas we detected, as previously described,31 an upregulation of *IL4R* mRNA in purified FL cells compared to normal $CD19^{pos}$ B cells and $CD19^{pos}$ $CD10^{pos}$ GC B cells (data not shown), CD124 was similarly expressed at the cell surface in FL cells and tonsil-derived GC B cells, indicating that the major tumor-associated event in the IL-4 pathway lies in the microenvironment. We detected significant *in vivo* activation of STAT6 in malignant B cells in contrast to normal GC B cells, in agreement with a functional IL-4-dependent signaling. Strikingly, STAT6-associated signal has been associated with other B-cell malignancies. In primary mediastinal large B-cell lymphoma, STAT6 is constitutively activated in both cell lines and primary samples32 whereas Hodgkin Reed-Sternberg cells produce autocrine IL-13 resulting in STAT6 activation in classical Hodgkin lymphoma. 33 However, even if IL-4 overexpression was already described in whole FL biopsies,22 we reinforced the belief that a paracrine secretion of IL-4 by tumor microenvironment could be involved in lymphomagenesis. STAT6 is a critical signaling molecule for IL-4-mediated protection of spontaneous and Fas-induced cell death in mice primary B cells.34 Moreover, even if few data are available on the direct effect of IL-4 on FL cells,35 in particular due to the lack of appropriate cell lines, STAT6 knockdown induces apoptosis in Hodgkin

lymphoma cell lines36 and IL-4 increases cell proliferation of GC-like diffuse large B-cell lymphomas (DLBCL) through STAT6 phosphorylation.24 A high proportion of genes overexpressed in FL B cells compared to normal $CD19^{pos}$ B cells, including *MME/CD10* , *BCL6* , and *MTA3* , corresponded in fact to GC-associated genes (data not shown). However, our approach, that compares purified FL cells, representing GC-derived neoplastic B cells, with normal B cells including both GC and non-GC derived B cells, is a suboptimal approach to characterize specifically FL B-cell features. One could therefore hypothesize that, since FL B cells gene profiling showed important molecular features of normal GC B cells and given that FL could evolve into GC-like DLBCL,37 the association of IL-4 overexpression and STAT6 activation could favor malignant B cell survival and proliferation. In addition, as previously described for GC-like DLBCL lines, IL-4 increased the expression of *GCET2/HGAL* in FL cells, and, given the role of HGAL in modulating GC B-cell motility,38 could thus contribute to the confinement of malignant B cells to the GC. Moreover, IL-4 drives macrophages toward a M2 phenotype endowed with immunoregulatory and proangiogenic properties, and several studies have indicated that tumors could educate recruited monocytes to exhibit a M2-like phenotype39 potentially implicated in the adverse prognostic value of a high number of tumor-associated macrophages in FL.13 Interestingly, the IL-4-specific target gene *IL4I1* was recently found as specifically expressed by malignant B cells in GC-derived B-cell lymphomas including FL, whereas no expression was observed in tumor cells of T/NK neoplasms, mantle cell lymphomas, or marginal zone lymphomas.22 Moreover, a significant correlation (P= 0.036) was found between high *IL4* mRNA expression and a low FLIPI score. However, a large cohort will be necessary to explore the prognostic value of IL-4/IL-4 target gene overexpression in FL.

Besides IL-4, several other cytokines were found to be overexpressed in FL_Env. In particular, we confirmed herein our previous results describing the induction of inflammatory cytokines, including *TNF* and *IFNG* , in FL microenvironment3 in agreement with the former detection of these two factors in FL-invaded LN using *in situ* hybridization or PCR experiments.40 ,41 The reason of the discrepancy between these data and the study of Calvo K. *et al* that reported a decrease of TNF-α and IFN-γ proteins in FL whole biopsies 22 is not clear. Of course, gene expression does not always correlate with protein expression but, since elevated levels of circulating TNF-α have been found in FL and DLBCL patients,42 another possible explanation could be the higher sensitivity of our purification-based method. In agreement, both *FASLG* and *GZMA* belonged to the 897-PS genelist defining the FL microenvironment, suggesting an activated T-cell signature in this disease.

Numerous studies have described several years ago that IL-4 is produced by the Th2 T-cell subset and promotes the Th2 polarization. In agreement with the overexpression of *IL4* in FL microenvironment, we reported an increased *GATA3/TBET* ratio in this disease, a finding generally interpreted as a bias in the Th1/Th2 balance. This result fit well with previous data showing that the few tumor-reactive effector T cells within FL tumors display a Th2 functional profile after *in vitro* stimulation.43 In addition, a mouse model of T-dependent lymphomagenesis has been recently developed where repeated infusions of idiotype-specific Th2 cells support the development of B-cell lymphoma, which could be conversely eradicated by Th1 cells.44 Finally, we detected a significant upregulation of *IL10* expression, another emblematic Th2 cytokine, within FL microenvironment. Interestingly, SNP in the *IL10* promoter were associated with increased risk for both DLBCL and FL.45 However, the segregation of helper T cells into unique highly specialized subsets has been recently challenged by several studies suggesting a common inductive history with intermediate stages exhibiting higher functional plasticity than previously believed.46 Gene expression profiling and analyses of knock-out mice models have first suggested that T_{FH} cells constitute a separate Th cell lineage with distinct developmental programming and specific effector functions, like providing help to B cells for their differentiation, into Ig-secreting cells.47 In addition, recent findings suggest that T_{FH} represent the normal counterpart of angioimmunoblastic T-cell lymphomas.47 ,48 Moreover, recent papers suggest that IL-4 secretion by lymphoid cells is highly related to T_{FH} cells in mice after helminth infection and in human inflamed tonsils25 –27 ,47 . We here demonstrate for the first time that chronically activated tumor-infiltrating $CXCR5^{hi}$ $ICOS^{hi}$ T_{FH} express high levels of IL-4 in FL suggesting major therapeutic implications.

IL-4 dependent STAT6 activation was reported to modulate the behavior of another very important $CD4^{pos}$ T-cell subset; *i.e* regulatory T cells (Treg). However, whereas initial studies clearly demonstrated that STAT6 directly represses TGFβ1-mediated *FOXP3* transcription and overrules inducible Treg differentiation,49 exogenous IL-4 conversely maintains *FOXP3* level in natural Treg and promotes their proliferation.50 In agreement, we found no correlation between the number of T_{FH} and the number of Treg within FL LN (data not shown).

In summary, we propose a new sensitive and specific gene profiling approach allowing the identification of genes involved in the crosstalk between malignant cells and their non-malignant microenvironment. Using this original and fully validated method, we revealed that FL microenvironment, along with P-STAT6 activated FL B cells, is characterized by a strong infiltration by T_{FH} cells displaying a specific activation profile characterized by the expression of IL-4. These findings could be very useful to better understand lymphoma biology and to develop effective targeted therapies in this still incurable disease.

Acknowledgements:

This work was supported by research fundings from the Institut National du Cancer (INCa libre 2005 – PL070), the Association pour la Recherche Contre le Cancer (ARC AO 2007), the Ligue Régionale contre le Cancer (AO 2004) and the Association pour le Développement de l'Hémato-Oncologie (ADHO). D.R. is supported by an INCa fellowship. The authors thank the "Centre de Ressources (CRB)-Santé" of

Rennes' hospital, Patrick Tas and Jean-Michel Picquenot for providing non-malignant and follicular lymph nodes, Christophe Ruaux for providing tonsil samples, and the “Institut Fédératif de Recherche (IFR)-140” of Rennes'University for cell sorting core facility.

Footnotes:

CONFLICT OF INTEREST The authors declare no competing financial interests.

Supplementary information is available at the Leukemia's website.

References:

- 1 . Bende RJ , Smit LA , van Noesel CJ . Molecular pathways in follicular lymphoma . Leukemia . 2007 ; Jan 21 : (1) 18 - 29
- 2 . Roulland S , Navarro JM , Grenot P , Milili M , Agopian J , Montpellier B . Follicular lymphoma-like B cells in healthy individuals: a novel intermediate step in early lymphomagenesis . J Exp Med . 2006 ; Oct 30 203 : (11) 2425 - 2431
- 3 . Ame-Thomas P , Maby-El Hajjami H , Monvoisin C , Jean R , Monnier D , Caulet-Maugendre S . Human mesenchymal stem cells isolated from bone marrow and lymphoid organs support tumor B-cell growth: role of stromal cells in follicular lymphoma pathogenesis . Blood . 2007 ; Jan 15 109 : (2) 693 - 702
- 4 . Travert M , Ame-Thomas P , Pangault C , Morizot A , Micheau O , Semana G . CD40 ligand protects from TRAIL-induced apoptosis in follicular lymphomas through NF-kappaB activation and up-regulation of c-FLIP and Bcl-xL . J Immunol . 2008 ; Jul 15 181 : (2) 1001 - 1011
- 5 . Nurieva RI , Chung Y , Hwang D , Yang XO , Kang HS , Ma L . Generation of T follicular helper cells is mediated by interleukin-21 but independent of T helper 1, 2, or 17 cell lineages . Immunity . 2008 ; Jul 29 : (1) 138 - 149
- 6 . King C , Tangye SG , Mackay CR . T follicular helper (TFH) cells in normal and dysregulated immune responses . Annu Rev Immunol . 2008 ; 26 : 741 - 766
- 7 . Ma CS , Suryani S , Avery DT , Chan A , Nanan R , Santner-Nanan B . Early commitment of naive human CD4(+) T cells to the T follicular helper (T(FH)) cell lineage is induced by IL-12 . Immunol Cell Biol . 2009 ; Nov–Dec 87 : (8) 590 - 600
- 8 . Lee AM , Clear AJ , Calaminici M , Davies AJ , Jordan S , MacDougall F . Number of CD4+ cells and location of forkhead box protein P3-positive cells in diagnostic follicular lymphoma tissue microarrays correlates with outcome . J Clin Oncol . 2006 ; Nov 1 24 : (31) 5052 - 5059
- 9 . Byers RJ , Sakhinia E , Joseph P , Glennie C , Hoyland JA , Menasce LP . Clinical quantitation of immune signature in follicular lymphoma by RT-PCR-based gene expression profiling . Blood . 2008 ; May 1 111 : (9) 4764 - 4770
- 10 . Carreras J , Lopez-Guillermo A , Fox BC , Colomo L , Martinez A , Roncador G . High numbers of tumor-infiltrating FOXP3-positive regulatory T cells are associated with improved overall survival in follicular lymphoma . Blood . 2006 ; Nov 1 108 : (9) 2957 - 2964
- 11 . Carreras J , Lopez-Guillermo A , Roncador G , Villamor N , Colomo L , Martinez A . High numbers of tumor-infiltrating programmed cell death 1-positive regulatory lymphocytes are associated with improved overall survival in follicular lymphoma . J Clin Oncol . 2009 ; Mar 20 27 : (9) 1470 - 1476
- 12 . Glas AM , Knoops L , Delahaye L , Kersten MJ , Kibbelaar RE , Wessels LA . Gene-expression and immunohistochemical study of specific T-cell subsets and accessory cell types in the transformation and prognosis of follicular lymphoma . J Clin Oncol . 2007 ; Feb 1 25 : (4) 390 - 398
- 13 . Farinha P , Masoudi H , Skinnider BF , Shumansky K , Spinelli JJ , Gill K . Analysis of multiple biomarkers shows that lymphoma-associated macrophage (LAM) content is an independent predictor of survival in follicular lymphoma (FL) . Blood . 2005 ; Sep 15 106 : (6) 2169 - 2174
- 14 . Alvaro T , Lejeune M , Salvado MT , Lopez C , Jaen J , Bosch R . Immunohistochemical patterns of reactive microenvironment are associated with clinicobiologic behavior in follicular lymphoma patients . J Clin Oncol . 2006 ; Dec 1 24 : (34) 5350 - 5357
- 15 . Taskinen M , Karjalainen-Lindsberg ML , Leppa S . Prognostic influence of tumor-infiltrating mast cells in patients with follicular lymphoma treated with rituximab and CHOP . Blood . 2008 ; May 1 111 : (9) 4664 - 4667
- 16 . Canioni D , Salles G , Mounier N , Brousse N , Keuppens M , Morchhauser F . High numbers of tumor-associated macrophages have an adverse prognostic value that can be circumvented by rituximab in patients with follicular lymphoma enrolled onto the GELA-GOELAMS FL-2000 trial . J Clin Oncol . 2008 ; Jan 20 26 : (3) 440 - 446
- 17 . de Jong D , Koster A , Hagenbeek A , Raemaekers J , Veldhuizen D , Heisterkamp S . Impact of the tumor microenvironment on prognosis in follicular lymphoma is dependent on specific treatment protocols . Haematologica . 2009 ; Jan 94 : (1) 70 - 77
- 18 . Dave SS , Wright G , Tan B , Rosenwald A , Gascoyne RD , Chan WC . Prediction of survival in follicular lymphoma based on molecular features of tumor-infiltrating immune cells . N Engl J Med . 2004 ; Nov 18 351 : (21) 2159 - 2169
- 19 . Glas AM , Kersten MJ , Delahaye LJ , Witteveen AT , Kibbelaar RE , Velds A . Gene expression profiling in follicular lymphoma to assess clinical aggressiveness and to guide the choice of treatment . Blood . 2005 ; Jan 1 105 : (1) 301 - 307
- 20 . Harjunpaa A , Taskinen M , Nykter M , Karjalainen-Lindsberg ML , Nyman H , Monni O . Differential gene expression in non-malignant tumour microenvironment is associated with outcome in follicular lymphoma patients treated with rituximab and CHOP . Br J Haematol . 2006 ; Oct 135 : (1) 33 - 42
- 21 . Carbonnelle-Puscian A , Copie-Bergman C , Baia M , Martin-Garcia N , Allory Y , Haioun C . The novel immunosuppressive enzyme IL4I1 is expressed by neoplastic cells of several B-cell lymphomas and by tumor-associated macrophages . Leukemia . 2009 ; May 23 : (5) 952 - 960
- 22 . Calvo KR , Dabir B , Kovach A , Devor C , Bandle R , Bond A . IL-4 protein expression and basal activation of Erk in vivo in follicular lymphoma . Blood . 2008 ; Nov 1 112 : (9) 3818 - 3826
- 23 . Schaffer A , Kim EC , Wu X , Zan H , Testoni L , Salamon S . Selective inhibition of class switching to IgG and IgE by recruitment of the HoxC4 and Oct-1 homeodomain proteins and Ku70/Ku86 to newly identified ATTT cis-elements . J Biol Chem . 2003 ; Jun 20 278 : (25) 23141 - 23150
- 24 . Lu X , Nechushtan H , Ding F , Rosado MF , Singal R , Alizadeh AA . Distinct IL-4-induced gene expression, proliferation, and intracellular signaling in germinal center B-cell-like and activated B-cell-like diffuse large-cell lymphomas . Blood . 2005 ; Apr 1 105 : (7) 2924 - 2932
- 25 . King IL , Mohrs M . IL-4-producing CD4+ T cells in reactive lymph nodes during helminth infection are T follicular helper cells . J Exp Med . 2009 ; May 11 206 : (5) 1001 - 1007
- 26 . Reinhardt RL , Liang HE , Locksley RM . Cytokine-secreting follicular T cells shape the antibody repertoire . Nat Immunol . 2009 ; Apr 10 : (4) 385 - 393
- 27 . Zaretsky AG , Taylor JJ , King IL , Marshall FA , Mohrs M , Pearce EJ . T follicular helper cells differentiate from Th2 cells in response to helminth antigens . J Exp Med . 2009 ; May 11 206 : (5) 991 - 999
- 28 . Rasheed AU , Rahn HP , Sallusto F , Lipp M , Muller G . Follicular B helper T cell activity is confined to CXCR5(hi)ICOS(hi) CD4 T cells and is independent of CD57 expression . Eur J Immunol . 2006 ; Jul 36 : (7) 1892 - 1903
- 29 . Brachtel EF , Washiyama M , Johnson GD , Tenner-Racz K , Racz P , MacLennan IC . Differences in the germinal centres of palatine tonsils and lymph nodes . Scand J Immunol . 1996 ; Mar 43 : (3) 239 - 247
- 30 . Allen CD , Ansel KM , Low C , Lesley R , Tamamura H , Fujii N . Germinal center dark and light zone organization is mediated by CXCR4 and CXCR5 . Nat Immunol . 2004 ; Sep 5 : (9) 943 - 952
- 31 . Husson H , Carideo EG , Neuberg D , Schultze J , Munoz O , Marks PW . Gene expression profiling of follicular lymphoma and normal germinal center B cells using cDNA arrays . Blood . 2002 ; Jan 1 99 : (1) 282 - 289
- 32 . Guiter C , Dusanter-Fourt I , Copie-Bergman C , Boulland ML , Le Gouvello S , Gaulard P . Constitutive STAT6 activation in primary mediastinal large B-cell lymphoma . Blood . 2004 ; Jul 15 104 : (2) 543 - 549
- 33 . Skinnider BF , Elia AJ , Gascoyne RD , Patterson B , Trumper L , Kapp U . Signal transducer and activator of transcription 6 is frequently activated in Hodgkin and Reed-Sternberg cells of Hodgkin lymphoma . Blood . 2002 ; Jan 15 99 : (2) 618 - 626
- 34 . Wurster AL , Rodgers VL , White MF , Rothstein TL , Grusby MJ . Interleukin-4-mediated protection of primary B cells from apoptosis through Stat6-dependent up-regulation of Bcl-xL . J Biol Chem . 2002 ; Jul 26 277 : (30) 27169 - 27175
- 35 . Schmitter D , Koss M , Niederer E , Stahel RA , Pichert G . T-cell derived cytokines co-stimulate proliferation of CD40-activated germinal centre as well as follicular lymphoma cells . Hematol Oncol . 1997 ; Nov 15 : (4) 197 - 207

- 36 . Baus D , Nonnenmacher F , Jankowski S , Doring C , Brautigam C , Frank M . STAT6 and STAT1 are essential antagonistic regulators of cell survival in classical Hodgkin lymphoma cell line . Leukemia . 2009 ; May 14
- 37 . Davies AJ , Rosenwald A , Wright G , Lee A , Last KW , Weisenburger DD . Transformation of follicular lymphoma to diffuse large B-cell lymphoma proceeds by distinct oncogenic mechanisms . Br J Haematol . 2007 ; Jan 136 : (2) 286 - 293
- 38 . Lu X , Chen J , Malumbres R , Cubedo Gil E , Helfman DM , Lossos IS . HGAL, a lymphoma prognostic biomarker, interacts with the cytoskeleton and mediates the effects of IL-6 on cell migration . Blood . 2007 ; Dec 15 110 : (13) 4268 - 4277
- 39 . Hagemann T , Biswas SK , Lawrence T , Sica A , Lewis CE . Regulation of macrophage function in tumors: the multifaceted role of NF-kappaB . Blood . 2009 ; Apr 2 113 : (14) 3139 - 3146
- 40 . Peuchmaur M , Emilie D , Crevon MC , Brousse N , Gaulard P , D'Agay MF . Interleukin-2 and interferon-gamma production in follicular lymphomas . Am J Clin Pathol . 1991 ; Jan 95 : (1) 55 - 62
- 41 . Warzocha K , Ribeiro P , Renard N , Bienvenu J , Charlot C , Coiffier B . Expression of genes coding for the tumor necrosis factor and lymphotoxin ligand-receptor system in non-Hodgkin's lymphomas . Cancer Immunol Immunother . 2000 ; Nov 49 : (9) 469 - 475
- 42 . Salles G , Bienvenu J , Bastion Y , Barbier Y , Doche C , Warzocha K . Elevated circulating levels of TNFalpha and its p55 soluble receptor are associated with an adverse prognosis in lymphoma patients . Br J Haematol . 1996 ; May 93 : (2) 352 - 359
- 43 . Anichini A , Mortarini R , Romagnoli L , Baldassari P , Cabras A , Carlo-Stella C . Skewed T-cell differentiation in patients with indolent non-Hodgkin lymphoma reversed by ex vivo T-cell culture with gammac cytokines . Blood . 2006 ; Jan 15 107 : (2) 602 - 609
- 44 . Zangani MM , Froyland M , Qiu GY , Meza-Zepeda LA , Kutok JL , Thompson KM . Lymphomas can develop from B cells chronically helped by idiotype-specific T cells . J Exp Med . 2007 ; May 14 204 : (5) 1181 - 1191
- 45 . Lan Q , Zheng T , Rothman N , Zhang Y , Wang SS , Shen M . Cytokine polymorphisms in the Th1/Th2 pathway and susceptibility to non-Hodgkin lymphoma . Blood . 2006 ; May 15 107 : (10) 4101 - 4108
- 46 . Fazilleau N , Mark L , McHeyzer-Williams LJ , McHeyzer-Williams MG . Follicular helper T cells: lineage and location . Immunity . 2009 ; Mar 20 30 : (3) 324 - 335
- 47 . Marafioti T , Paterson JC , Ballabio E , Chott A , Natkunam Y , Rodriguez-Justo M . The inducible T-cell co-stimulator molecule is expressed on subsets of T cells and is a new marker of lymphomas of T follicular helper cell-derivation . Haematologica . Mar 95 : (3) 432 - 439
- 48 . de Leval L , Rickman DS , Thielen C , Reynies A , Huang YL , Delsol G . The gene expression profile of nodal peripheral T-cell lymphoma demonstrates a molecular link between angioimmunoblastic T-cell lymphoma (AITL) and follicular helper T (TFH) cells . Blood . 2007 ; Jun 1 109 : (11) 4952 - 4963
- 49 . Takaki H , Ichiyama K , Koga K , Chinen T , Takaesu G , Sugiyama Y . STAT6 Inhibits TGF-beta1-mediated Foxp3 induction through direct binding to the Foxp3 promoter, which is reverted by retinoic acid receptor . J Biol Chem . 2008 ; May 30 283 : (22) 14955 - 14962
- 50 . Pillemer BB , Qi Z , Melgert B , Oriss TB , Ray P , Ray A . STAT6 activation confers upon T helper cells resistance to suppression by regulatory T cells . J Immunol . 2009 ; Jul 1 183 : (1) 155 - 163

Figure 1

Microarray analysis and « FL specific interface » definition

(A) Cluster diagrams of B and non-B cell compartments in FL and non-malignant lymph nodes. Hierarchical clustering of the $CD19^{pos}$ compartments (Left Panel) and $CD19^{neg}$ $CD22^{neg}$ compartments (Right Panel) issued from FL lymph nodes (FL_B or FL_Env) and non-malignant lymph nodes (NEG_B or NEG_Env). The relative level of gene expression is depicted according to the shown color scale. To the right of the dendrogram, the positionning of the genes making up the T_{FH} signature. (B) Schematic approach to identify host-tumor interface gene expression. *Left Panel* : Microarray signature overlapping of the four B and non-B, follicular and non-malignant compartments to define the FL interface (4127 PS), the normal interface (2308 PS), FL-specific B signature (886 PS) and FL-specific non-B environment signature (897 PS). *Middle Panel* : FL specific interface 1 is defined as the FL interface cleared of probesets overlapping with the normal interface; interface 2 is defined as the addition of the FL-specific B and FL-specific non-B signatures. *Right Panel* : The so called "FL specific interface" defined the most relevant genes involved in the FL and microenvironment interface, represented by the probesets which overlapped between FL-specific interface 1 and interface 2.

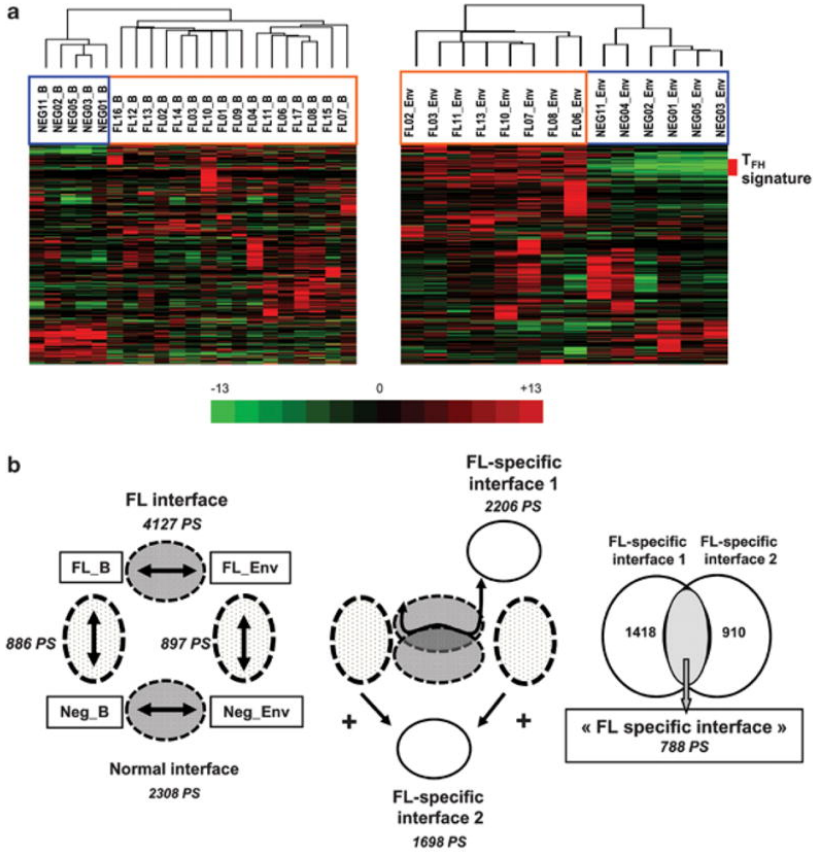

Figure 2

Specific expression of functional IL-4 and PSTAT6 in FL microenvironment

(A) Gene expression of *IL4* in non-B cell fractions. RQ-PCR quantification of *IL4* in CD19^{neg} CD22^{neg} fractions obtained from FL lymph nodes (FL_Env), non-malignant lymph nodes (NEG_Env) and tonsils (TONS_Env). The arbitrary value of 1 was assigned to the median expression of NEG_Env. (B) CD124 membrane expression on B cells. Expression of CD124 on CD19^{pos} B cells from FL lymph nodes (FL_B) and non-malignant lymph nodes (NEG_B), as well as CD19^{pos} CD10^{pos} germinal center B cells from tonsils (TONS_GC B) was analyzed as the ratio of mean fluorescence intensity (rMFI). (C) Immunohistochemical staining of Phospho STAT6: 1/a single P-STAT6^{pos} cell with nuclear staining (brown) is observed within the GC of a reactive tonsil with follicular hyperplasia (arrow), 2 and 3/a significant number of P-STAT6^{pos} cells are present in neoplastic follicles in FL, consisting of clusters predominating at the periphery of follicles (C2, see details in insert) or scattered positive cells (C3); as shown in insert (C3), P-STAT6^{pos} cells (brown) are CD20^{pos} (red) B cells. Original magnifications: x100 (C2), x200 (C1, C3), x400 (inserts). (D) Gene expression of *GCET2/HGAL* in B cells. RQ-PCR quantification of *GCET2/HGAL* in purified CD19^{pos} fractions from FL lymph nodes (FL_B) cultured with (IL-4) or without (CTL) IL-4 for 2 days. The arbitrary value of 1 was assigned to the median expression of unstimulated (CTL) FL_B. (*P <0.05, ***P <0.001).

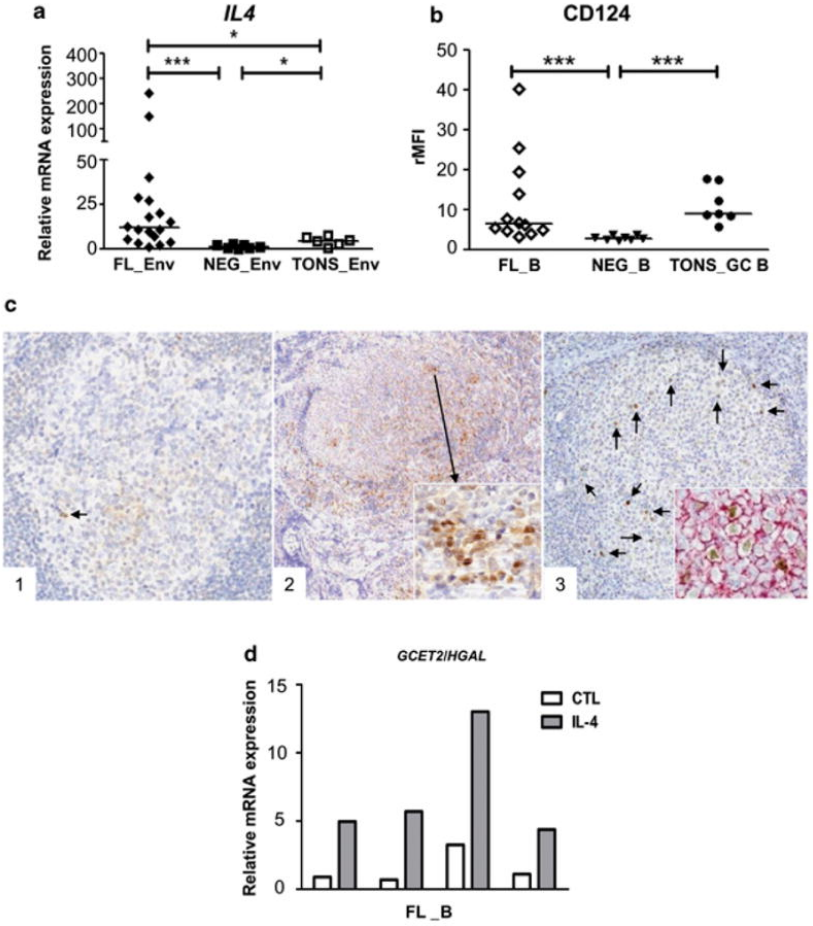

Figure 3

Classification of FL_Env displaying various *IL4* expressions based on the T_{FH} signature

Hierarchical clustering of FL_Env was performed on the selected genes making up the T_{FH} signature. The FL_Env cases were assigned to IL4^{low} (*IL4^{lo}*) or IL4^{high} (*IL4^{hi}*) expression according to their relative mRNA expression compared to NEG_Env (see Materials and Methods).

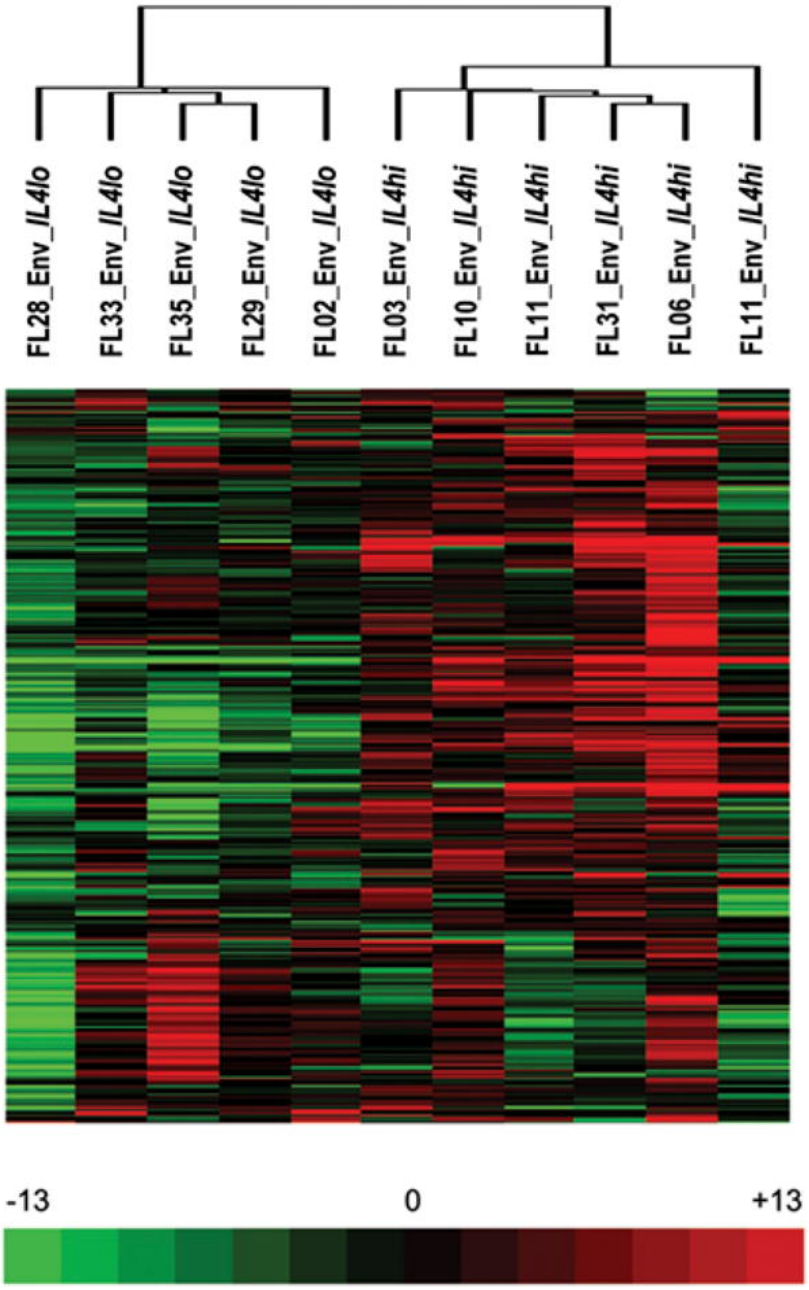

Figure 4

Specific expression of IL-4 by FL-infiltrating T_{FH}

(A) Strategy for flow cytometry analysis and cell sorting of $T_{FH\ cells}$. T_{FH} are defined as $CXCR5^{hi}$ $ICOS^{hi}$ cells within $CD4^{pos}$ $CD25^{neg}$ T cells. (B) Quantification of the T_{FH} cell compartment. Enumeration by flow cytometry of $CXCR5^{hi}$ $ICOS^{hi}$ $CD25^{neg}$ cells within $CD4^{pos}$ T cells in FL lymph nodes, non-malignant (NEG) lymph nodes, and tonsils (TONS). (C) Double staining of P-$STAT6^{pos}$ cells in FL samples. 1/P-$STAT6^{pos}$ cells (brown) are in close contact with $CD5^{pos}$ T cells (red), 2/numerous $PD1^{pos}$ cells (brown) within a neoplastic follicle are seen among P-$STAT6^{pos}$ (red) cells; insert illustrates P-$STAT6^{pos}$ cells at the vicinity of $PD1^{pos}$ cells. Original magnification, x200 (C2), x400 (C1, insert). (D) Gene expression of *IL4* in T_{FH} versus nonT_{FH} microenvironment. RQ-PCR quantification of *IL4* in T_{FH} and T_{FH} -depleted B cell-depleted cell compartment (Env non T_{FH}) cell sorted from FL lymph nodes (7 FL_T_{FH} and 4 FL_Env nonT_{FH}) and tonsils (7 TONS_T_{FH} and 4 TONS_Env nonT_{FH}). The arbitrary value of 1 was assigned to the median expression obtained for 4 $CD19^{neg}$ $CD22^{neg}$ fractions from FL lymph nodes. Bar represents the median. (***P*< 0.01; ****P*< 0.001)